

Intracluster Planetary Nebulae in the Virgo Cluster III: Luminosity of the Intracluster Light and Tests of the Spatial Distribution

John J. Feldmeier^{1,2,3}

*Department of Astronomy and Astrophysics, Penn State University, 525 Davey Lab,
University Park, PA 16802*

johnf@bottom.astr.cwru.edu

Robin Ciardullo¹

*Department of Astronomy and Astrophysics, Penn State University, 525 Davey Lab,
University Park, PA 16802*

rbc@astro.psu.edu

George H. Jacoby

*WIYN Observatory
P.O. Box 26732, Tucson, AZ 85726*

gjacoby@wiyn.org

and

Patrick R. Durrell

*Department of Astronomy and Astrophysics, Penn State University, 525 Davey Lab,
University Park, PA 16802*

pdurrell@astro.psu.edu

ABSTRACT

¹Visiting Astronomer, Kitt Peak National Observatory, National Optical Astronomy Observatory, which is operated by the Association of Universities for Research in Astronomy, Inc. (AURA) under cooperative agreement with the National Science Foundation.

²present address: Department of Astronomy, Case Western Reserve University, 10900 Euclid Ave, Cleveland, OH 44106

³NSF Astronomy and Astrophysics Postdoctoral Fellow

Intracluster planetary nebulae are a useful tracer of the evolution of galaxies and galaxy clusters. We analyze our catalog of 318 intracluster planetary nebulae candidates found in 0.89 square degrees of the Virgo cluster. We give additional evidence for the great depth of the Virgo cluster’s intracluster stellar population, which implies that the bulk of the intracluster stars come from late-type galaxies and dwarfs. We also provide evidence that the intracluster stars are clustered on the sky on arcminute scales, in agreement with tidal-stripping scenarios of intracluster star production. Although significant systematic uncertainties exist, we find that the average fraction of intracluster starlight in the Virgo is $15.8\% \pm 3.0(\text{statistical}) \pm 5.0(\text{systematic})$, and may be higher if the intracluster stars have a large spatial line-of-sight depth. We find that the intracluster star density changes little with radius or projected density over the range surveyed. These results, along with other intracluster star observations, imply that intracluster star production in Virgo is ongoing and consistent with the cluster’s known dynamical youth.

Subject headings: galaxies: clusters: general — galaxies: clusters: individual (Virgo) — galaxies: interactions — galaxies: kinematics and dynamics — planetary nebulae: general

1. Introduction

The concept of intracluster starlight was first proposed by Zwicky (1951), who claimed to detect excess light between the galaxies of the Coma cluster. Follow-up photographic searches for intracluster luminosity in Coma and other rich clusters (e.g., Welch & Sastry 1971; Melnick, White & Hoessel 1977, see Víchez-Gómez 1999 and Feldmeier 2000 for reviews) produced mixed results, and it was not until the advent of CCDs that more precise estimates of the amount of intracluster starlight were made (e.g., Uson, Boughn, & Kuhn 1991; Víchez-Gómez, Pelló, & Sanahuja 1994; Bernstein et al. 1995; Gonzalez et al. 2000). However, even these modern measurements carry a substantial uncertainty, due to the extremely low surface brightness of the phenomenon. Typically the brightest intracluster regions are less than $\sim 1\%$ of the brightness of the night sky in the V band (e.g., Feldmeier et al. 2002), and measurements of this luminosity must also contend with the problems presented by scattered light from nearby bright objects and the contribution of faint discrete sources.

Recently, a great deal of progress has been made in the study of intracluster light (ICL). Our ability to measure the ICL in Abell clusters has grown to the point that reliable surface photometry is now possible at levels several magnitudes (0.1% to $.01\%$ in the V and I bands)

lower than that of the sky (e.g., Tyson, Kochanski & dell’Antonio 1998; Gonzalez et al. 2000; Feldmeier et al. 2002). These studies are making it possible to study the evolution of the ICL as a function of redshift, cluster substructure, galactic density, and galactic morphology. Meanwhile, high-resolution N-body models now have the ability to follow hundreds of interacting cluster galaxies within a cosmological context (Moore et al. 1996; Dubinski 1998; Napolitano et al. 2003; Mihos et al. 2004b; Willman et al. 2004). These high-quality simulations are making testable predictions concerning the production of intracluster light. When combined with earlier and recent semi-analytic studies (Gallagher & Ostriker 1972; Merritt 1983; Richstone & Malumuth 1983; Miller 1983; Merritt 1984; Muccione & Ciotti 2004) there is now sufficient theoretical insight to begin to interpret the observations.

Another major advance in the study of the ICL is our growing ability to study individual intracluster objects such as globular clusters (West et al. 1995; Jordán et al. 2003) and in particular, individual intracluster stars, specifically planetary nebulae (IPNe), red giants (IRGs; Ferguson, Tanvir, & von Hippel (1998); Durrell et al. (2002)) and supernovae (ISNe; Gal-Yam et al. (2003)). Perhaps the most useful of these objects are the planetaries. IPNe have several unique features that make them ideal for probing intracluster starlight (for a complete review, see Feldmeier 2003). In the light of [O III] $\lambda 5007$, planetary nebulae (PNe) are extremely luminous, and can be observed out to distances of ~ 25 Mpc with present day telescopes. Planetary nebulae are also excellent tracers of stellar luminosity (Ciardullo, Jacoby, & Ford 1989; Ciardullo et al. 1989), and their number counts can be scaled to produce estimates of the total amount of unseen light. In addition, through the [O III] $\lambda 5007$ planetary nebula luminosity function (PNLF), PNe are precise distance indicators (Jacoby et al. 1992; Ciardullo 2002b); therefore, the observed shape of the PNLF provides information on the line-of-sight distribution of the intracluster stars. Finally, since the [O III] $\lambda 5007$ emission is in a narrow line, IPN velocities can be determined via moderate ($\lambda/\Delta\lambda \sim 2000$) resolution spectroscopy, making kinematical studies of the ICL possible.

In this paper, we utilize the 318 IPN candidates detected in our photometric survey of Virgo (Feldmeier, Ciardullo, & Jacoby 1998; hereafter Paper I; Feldmeier et al. 2003a; hereafter Paper II) to place limits on the amount and distribution of intracluster starlight in that cluster. In §2, we review the observations and reduction procedures which produced the IPN catalog. In §3, we use the IPN data to estimate the three-dimensional structure of Virgo’s diffuse stellar component. We compare the distribution of ICL to that of the galaxies and the hot intracluster medium, and present evidence that Virgo’s IPNe are clumped on small scales. In §4, we compute the total amount of intracluster starlight that must be present in Virgo, discuss the systematic uncertainties present in this number, and compare the large scale distribution of IPNe with that of two common parameters of cluster dynamical evolution: cluster radius and projected galaxy density. We discuss the implications of our

results in §5 and combine our data with the observation of intracluster red giants, to place constraints on the population of the intracluster stars and on their origins. We stress that not all of the 318 candidates are genuine IPNe: we estimate (Ciardullo et al. 2002a) that $\sim 20\%$ of the IPN candidates are likely background objects that are themselves of considerable scientific interest (e.g., Kudritzki et al. 2000; Rhoads et al. 2000; Stern et al. 2000).

For this paper, we adopt ~ 15 Mpc as the distance to the Virgo cluster core. This number is consistent with the PNLF distances to the elliptical galaxies of the core (Jacoby, Ciardullo, & Ford 1990; Ciardullo et al. 1998), and enables us to compare our IPN measurements directly with the PNLF observations of ellipticals. We note that such a distance is ~ 0.7 Mpc smaller than the mean distance estimated from Cepheid variables by the *HST* Distance Scale Key Project and others (Pierce et al. 1994; Saha et al. 1997; Freedman et al. 2001). Such a discrepancy is not serious, especially since there is growing evidence that the ellipticals of Virgo are not necessarily at the same distance as the spirals (West & Blakeslee 2000; Drinkwater, Gregg, & Colless 2001). Additionally, the median distances of the two methods are consistent within the errors, and the difference in the mean is solely due to the most distant galaxy NGC 4639 ($D = 20.8^{+2.8}_{-2.5}$; Freedman et al. 2001). In any case, all quantities in this paper that are dependent on this distance will be expressed as a function of D_{15} , where $D_{15} = D_{\text{VirgoCore}}/15$ Mpc.

2. Observations

The detection, photometry, and astrometry of the 318 IPN candidates were reported in full in Paper II. Here, we briefly summarize the results. The images for this survey were taken over the course of three observing runs from March 1997 to March 1999 at the Kitt Peak National Observatory (KPNO) using the 4 m telescope and the Prime Focus CCD camera for runs 1 and 2 (PFCCD) and the NOAO MOSAIC I imager (MOSAIC; Muller et al. 1998) for run 3. The data are composed of images taken through an [O III] $\lambda 5007$ narrow-band filter, and a medium-band continuum filter. IPN candidates appear as point sources in the former filter, but disappear in the latter filter. The IPN candidates were detected semi-automatically using two separate methods, and objects in, or adjacent to, Virgo cluster galaxies have been culled from our sample. In addition, any source known to be present in the continuum, or shown to be a background galaxy through follow-up spectroscopy has been removed. We stress, however, that only 10% of the sources have follow-up spectra, and those spectra that do exist have low signal-to-noise. We will return to this point later.

After identifying the IPN candidates, we determined [O III] $\lambda 5007$ magnitudes by comparing their fluxes to spectrophotometric standards defined by Stone (1977) and Massey

et al. (1988). We define our [O III] $\lambda 5007$ magnitudes in the same way as Jacoby (1989):

$$m_{5007} = -2.5 \log F_{5007} - 13.74 \quad (1)$$

where F_{5007} is in $\text{ergs cm}^{-2} \text{ s}^{-1}$. Equatorial coordinates were obtained for each intracluster planetary nebula candidate by comparing its position to those of USNO-A 2.0 astrometric stars (Monet 1998; Monet et al. 1996) on the same frame. The magnitude limit of each frame was determined by adding artificial stars to the data and estimating the recovery fraction as a function of magnitude (e.g., Stetson 1987; Bolte 1989; Harris 1990). To be conservative, the 90% completeness level has been adopted as the limiting magnitude for each field. The field locations are shown graphically in Paper II, Figure 1. The resulting luminosity functions for each field, binned into 0.2 magnitude intervals, are shown in Figure 1. The original data for Field 1 has been superseded by the Field 7 results (Paper II).

3. The Spatial Distribution of Intracluster Starlight

The first step towards understanding the mechanisms which produce intracluster stars is to compare the stars’ spatial distribution with that of the better-studied components of galaxy clusters: the cluster galaxies, the hot intracluster gas, and the invisible dark matter, which dominates the total mass. For example, if most intracluster stars are removed early in a cluster’s lifetime (Merritt 1984), the distribution of this diffuse component will be smooth and follow the cluster potential. However, if a significant portion of the stars are removed at late epochs via galaxy encounters and tidal stripping (e.g., Richstone & Malumuth 1983; Moore et al. 1996), then the ICL should be clumpy and have a non-relaxed appearance. In particular, the “harassment” models of Moore et al. (1996) and Moore, Lake, & Katz (1998) first predicted that many intracluster stars will exist in long (~ 2 Mpc) tidal tails, which may maintain their structure for Gigayears. Since Virgo is thought to be dynamically young (Tully & Shaya 1984; Binggelli, Popescu & Tammann 1993 and references within), it is possible that such structures are still present and observable.

Since planetary nebulae closely follow the distribution of starlight in galaxies (e.g., Ciardullo, Jacoby, & Ford 1989; Ciardullo et al. 1989), they should be an ideal tracer of Virgo’s intracluster population. Here, we detail our efforts to determine the spatial distribution of the intracluster stars through the analysis of the IPN data.

3.1. The Depth of Intracluster Starlight in the Virgo cluster

From theory (e.g., Dopita et al. 1992; Stanghellini 1995; Méndez & Soffner 1997), and observations (e.g., Ciardullo et al. 2002b, and references therein), it has been shown that bright planetary nebulae follow a well-defined luminosity function in the light of [O III] $\lambda 5007$. In particular, the [O III] planetary nebula luminosity function (PNLF) at the brightest magnitudes is well fit by an exponential function with a sharp bright-end cutoff M^* , i.e.,

$$N(M) \propto e^{0.307M} \{1 - e^{3(M^* - M)}\} \quad (2)$$

Since there is no reason to believe that IPNe would not also follow the PNLf, it is possible to use this cutoff to probe distances in the intracluster environment. However, an implicit assumption of the PNLf method is that all the PNe that make up the observed luminosity function are effectively at the same distance (e.g., in a normal galaxy). In a cluster such as Virgo, the finite depth of the cluster can distort the PNLf, as IPNe at many different distances can contribute to the observed luminosity function. In this case, the PNLf of the IPNe will be the convolution of the intrinsic luminosity function and the density function of the IPNe along the line-of-sight. Thus, the shape of the observed luminosity function can be exploited to learn about the three-dimensional distribution of the ICL.

Unfortunately, deriving the complete line-of-sight distribution is not trivial. Mathematically, the function is:

$$O(m) = [(\rho(\mu) * N(M)) + C(m)] * E(m) \quad (3)$$

where $O(m)$ is the final observed luminosity function, $N(M)$ is the empirical PNLf, $\rho(\mu)$ is the density of intracluster PNe as a function of distance modulus, μ , $C(m)$ is the apparent luminosity function of any contaminating objects, and $E(m)$ is the photometric error function of the observations. Although the intrinsic luminosity function is known and the error function is, in principle, derivable from our photometry (this function is not necessarily a Gaussian; Stetson & Harris 1988), the luminosity function of the contaminants is not currently well-known. This places a fundamental limit on our ability to measure $\rho(\mu)$. With an improved estimate of $C(m)$, we will be able to do a much better job at constraining this function.

For the present, we focus on a much simpler case: the magnitude of the brightest IPN candidate in each field. Given the empirical PNLf, there is a maximum absolute magnitude M^* , that a PNe may have in the light of [O III] $\lambda 5007$. If we assume that the brightest observed IPN candidate in each field has this absolute magnitude, we can derive its upper limit distance, and therefore estimate the distance to the front edge of the Virgo intracluster population. For this paper, we adopt a value of M^* of -4.51 (Ciardullo et al. 2002b).

Figure 2 displays our upper limit distances, along with similar limits found by other authors using similar techniques (Ciardullo et al. 1998; Arnaboldi et al. 2002; Okamura et al. 2002). Field 8 has been excluded from the analysis, since the IPN density of the field is consistent with zero (Paper II). The extraordinary IPN candidate I-33 of Okamura et al. (2002), which is over 0.8 magnitudes brighter than all other objects in our survey, has also been omitted from the diagram. For comparison, Figure 2 also shows the Cepheid-based distances to six Virgo spirals (Pierce et al. 1994; Saha et al. 1997; Freedman et al. 2001) and the PNLf distances of six Virgo early-type galaxies (Jacoby, Ciardullo, & Ford 1990; Ciardullo et al. 1998). Note that Virgo is known to have a complex structure with at least two main subclusters: cluster A, which is dominated by the giant elliptical M87 (and contains the background M84/M86 subgroup; Böhringer et al. 1994; Schindler, Binggeli, & Böhringer 1999), and cluster B, which contains the giant elliptical M49 (Binggeli, Tammann & Sandage 1987). The respective subclusters for each field are labeled in the figure.

Several results are apparent from the data. First, there is a general offset in the upper limit distances between IPN observations in subclusters A and B. According to our data, the front of subcluster A is at a distance of 12.7 ± 0.4 Mpc, while subcluster B begins at 14.1 ± 0.8 Mpc. These distance estimates use all the datasets and include all possible systematic errors common to the PNLf method (see Ciardullo et al. 2002b for a discussion of these systematic effects). If we take an average of the brightest m_{5007} magnitudes of our fields (2–7, and the M87 field of Ciardullo et al. 1998) weighted solely by the photometric errors, we find that the average magnitude of the brightest IPNe candidates in subcluster A is $m_{5007} = 25.87 \pm 0.03$, while that of the brightest IPNe in subcluster B is $m_{5007} = 26.20 \pm 0.06$, corresponding to a difference at the 4.9σ level. If, instead of using just the brightest IPNe, we fit the data to the empirical PNLf using the method of maximum likelihood (Ciardullo et al. 1989), then the upper limit distance to each field decreases by ~ 0.7 Mpc (Field 4 excepted, since that region does not contain enough planetaries for a reliable PNLf analysis). This systematic shortening of the distances is expected, since it is more probable that the brightest IPNe have magnitudes slightly fainter than M^* , rather than precisely at M^* . Nevertheless, the analysis confirms the fact that intracluster stars of subclump B is substantially more distant than those of subclump A.

The systematic difference between the upper limit distances is most likely due to the internal geometry of Virgo: observations by Yasuda, Fukugita, & Okamura (1997) and Federspiel, Tammann, & Sandage (1998) demonstrate that the galaxies of subcluster B have a mean distance modulus ~ 0.4 mag more distant than those of subcluster A. Moreover, the two discrepant points in this relation, Field 4 and Subaru 1, can be easily explained through other means. Field 4 only has two objects in its photometrically complete sample, so small number statistics affect its distance determination. (The probability of one of these PNe

being within ~ 0.2 mag of M^* is only $\sim 30\%$.) Subaru 1, on the other hand, is centered on the M84/M86 subclump of cluster A, and this system is known to lie ~ 0.2 mag behind the Virgo core (e.g., Binggeli, Popescu, & Tammann 1993; Böhringer et al. 1994; Schindler, Binggeli, & Böhringer 1999; Jerjen, Binggeli & Barazzi 2003). Therefore, the upper limit distance of Subaru 1 probably reflects the distance to this background subgroup, and not the Virgo cluster as a whole.

A second property which is obvious from Figure 2 is that the intracluster distance to subcluster A is clearly much closer than the 15 Mpc assumed for the cluster core. As has been pointed out previously (Ciardullo et al. 1998; Paper I; Arnaboldi et al. 2002), this is due to a selection effect: it is much easier to detect an IPNe located on the front edge of the cluster than one located on the back edge. Thus, our upper limit IPN distances represent measurements to the front edge of Virgo’s ICL, not the system’s mean distance. Nevertheless, the depth implied from our measurements is remarkable. If we take the data at face value, then the IPN distribution has a line-of-sight radius of $4.2 + (15 * (D_{15} - 1))$ Mpc. If we compare this radius to the classical radius of Virgo on the sky ($\sim 6^\circ 0$, or $\sim 1.6D_{15}$ Mpc; Shapley & Ames 1926; de Vaucouleurs & de Vaucouleurs 1973; Binggeli, Tammann & Sandage 1987) we find that the Virgo cluster is more than 2.6 times as deep as it is wide. Virgo is nowhere near a spherical cluster: it contains considerable substructure, and is elongated significantly along our line of sight.

Our inferred depth for the Virgo Cluster is much greater than the ~ 2 Mpc value associated with the early-type galaxies of the cluster’s core (i.e., Jacoby, Ciardullo, & Ford 1990; Tonry et al. 2001; Neilsen & Tsvetanov 2000). On the other hand, this depth agrees extremely well with that derived from Tully-Fisher observations of the cluster’s spirals. According to Yasuda, Fukugita, & Okamura (1997) and Solanes et al. (2002), Virgo is highly elongated along the line-of-sight, with a width-to-depth ratio of $\sim 1:4$, and an overall depth of ~ 10 Mpc. Much of this depth lies background to the core ellipticals, but the line of spirals does extend into the foreground. This conclusion is strengthened by the discovery of hydrogen deficient spirals on the outskirts ($R > 4$ Mpc) of Virgo, which have likely moved through the cluster core (Sanchis et al. 2002). Moreover, it is also in agreement with the results of Jerjen, Binggeli, & Barazza (2004), who find a Virgo Cluster depth of 6 Mpc from SBF measurements of its dwarf ellipticals. Since simulations (Moore, Lake, & Katz 1998; Dubinski, Murali, & Ouyed 2000) show that the majority of intracluster stars are ejected into orbits similar to that of their parent galaxies, our measurements imply that the bulk of Virgo’s intracluster stars originate in late-type galaxies and dwarfs. If IPNe were derived from elliptical galaxies, the depth of the ICL would be much less.

A complication from this analysis is that we might be inadvertently combining two

different components of ICL together in our analysis: a “core” component associated with the elliptical galaxies, and a component of stars removed from galaxy-galaxy interactions in the infalling regions of Virgo. We believe this to be unlikely for a number of reasons. First, modern models of intracluster star production imply that the bulk of intracluster stars are released when their parent galaxies and groups pass through pericenter (see Mihos 2004a; Willman et al. 2004 for some graphical examples). The relative amount of intracluster star production is much less on the outskirts of a galaxy cluster. Second, if such a component existed, the lower relative velocities of such encounters would imply that there would still be luminous “parent” galaxies nearby our IPN fields (100-200 kpc) in the foreground, assuming that the interactions happened 1-2 Gyr ago. This does not appear to be the case (see §4.2).

Finally, there is independent evidence that galaxies that have traveled through the cluster core can return to radial distances of ~ 4 Mpc. As mentioned previously, observations of H I deficient spiral galaxies show depths that are even larger than those derived from the IPNe (Sanchis et al. 2002). Since the accepted explanation for H I deficiency is ram pressure stripping by the hot gas in the cluster core (Gunn & Gott 1972), the existence of these galaxies imply that at least some Virgo objects have extended radial orbits. Moreover, although the apocenter distances of these galaxies are somewhat uncertain, due to errors in their Tully-Fisher distances and other effects (Sanchis et al. 2002), there is good reason to believe that a depth of ~ 4 Mpc is not unreasonable. Using standard cosmological simulations, Mamon, Sanchis, Salvador-Solé, & Solanes (2004) found that the maximum rebound radius reached by infalling galaxies is roughly between 1 and 2.5 times the cluster virial radii. When they scaled this result to the Virgo Cluster, Mamon, Sanchis, Salvador-Solé, & Solanes (2004) found a corresponding rebound depth of 4.1 Mpc, remarkably similar to that found for the IPN distribution. Although the precise agreement between the infall models and the IPN distances is probably fortuitous, it does suggest that our measured depth for the intracluster stars is plausible. Models by Moore, Diemand, & Stadel (2004), which predict a maximum orbital radius of ~ 3 virial radii, further support our result.

ICL comparisons with the hot intracluster medium are less straightforward. Multiple studies with *ROSAT* and *ASCA* (Bohringer et al. 1994; Schindler, Binggeli, & Böhringer 1999; Shibata et al. 2001, and references therein), demonstrate that the X-ray emission from Virgo’s intracluster medium extends ~ 4 to 5 degrees ($\sim 1.2D_{15}$ Mpc) from M87, and generally follows the galaxy distribution. However, the line-of-sight depth of this component is unclear. Although intracluster gas is dissipative, and the majority of clusters are only mildly aspherical in their X-ray distributions (Mohr et al. 1995), there are cases where the X-ray contours are considerably elongated (up to a factor of three in depth; Mohr et al. 1995). Therefore, although the data suggest that the IPNe are more widely distributed in depth than the gaseous intracluster medium, this cannot be proven.

Our conclusions above have two caveats. First, from the spectroscopic observations of Kudritzki et al. (2000) and Freeman et al. (2000), it is clear that there are contaminating objects as bright as $m_{5007} = 25.8$ present within our Virgo survey data. Therefore, the upper limits displayed in Figure 2 could be affected by these interlopers. However, there are a number of reasons to believe that our estimates are accurate. The most powerful argument in support of our distance estimates is the magnitude offset between the results from subclusters A and B. It is difficult to see how this difference could be caused by background contaminating objects, since to first order, these objects are scattered uniformly across the sky. Second, given a contamination probability of $\sim 20\%$ (Freeman et al. 2000; Ciardullo et al. 2002a), it is unlikely that the majority of the bright IPN candidates are background galaxies. Finally, the spectroscopic observations of Ciardullo et al. (2002a) definitively show that the brightest IPN candidates in front of M87 have [O III] $\lambda 5007$ emission, and are not background objects. From these data, the ICL extends at least ~ 2 Mpc in front of Virgo’s central galaxy. Similar results have been found by narrow-band $H\alpha$ imaging and limited spectroscopic follow-up by Okamura et al. (2002) and Arnaboldi et al. (2003).

A more troubling issue concerns the possibility of intracluster H II regions. Gerhard et al. (2002) recently discovered an isolated H II region in the outer halo of NGC 4388 or possibly in intracluster space. Such objects would emit [O III] $\lambda 5007$, and, if smaller than ~ 50 pc in size, would be indistinguishable from IPNe without deep continuum images or Balmer-line spectroscopy. Fortunately, such objects are rare. Even if these objects are distributed throughout Virgo’s intracluster space, then the density reported by Gerhard et al. (2002) implies a contamination fraction of only $\sim 3\%$. Additionally, Vollmer & Huchtmeier (2003) claim that the isolated H II region discovered by Gerhard et al. (2002) was formed from gas that was ram-pressure stripped from NGC 4388, and now is falling back into the galaxy. If this is correct, it is less likely that large numbers of isolated H II regions will be found far away from their parent galaxies (however, see Ryan-Weber et al. 2003 for some examples). Spectroscopic observations of the brightest IPNe would remove any uncertainty.

3.2. The Angular Distribution of the Intracluster Stars

Another useful way to probe the distribution of Virgo’s intracluster light is through the locations of the IPNe on the sky. These are shown in Figure 3. For reference, at the distance of Virgo, $1'$ corresponds to $\sim 4.36D_{15}$ kpc. Studying the IPNe in this way allows us to use more of the IPN candidates in the analysis and investigate the intracluster light distribution on smaller spatial scales. It is obvious from the figure that at least some of our fields contain significant evidence of substructure. For example, of the 16 IPNe of Field 2, none are present

in the bottom third of the CCD frame. This segregation is not instrumental – none of the other fields exhibit that property. From simple binomial statistics, the probability of the bottom third of the field being empty is less than $\sim 0.15\%$.

Of course, the eye can be fooled, and *a posteriori* statistics are of questionable validity. What is needed is an unbiased statistical test of the spatial distribution of IPN candidates. The traditional approach for such an analysis is the two-point angular correlation function (Peebles 1980), which is defined as the joint probability of finding two objects in two particular elements of solid angle on the sky. Since the accuracy of this method depends on the number of object pairs in the sample, the limited of IPN candidates in Fields 2–6 make this statistic too noisy for diagnostic purposes.

A simpler procedure that requires less data is quadrat analysis (see Diggle 1983 and references therein). This method is a two-dimensional analog to the more common three dimensional “counts-in-cells” test used in cosmological surveys (Peebles 1980), and was first used in studies of galaxy clusters by Abell (1961). Like the two point correlation function, quadrat analysis compares the observed IPN distribution against a random distribution. Unlike correlation functions, however, quadrat analysis has the ability, at least in theory, to test for the presence of sheets and filaments.

The principle of quadrat analysis is simple. If one divides a field into m regions, and the objects are distributed randomly, then the number of objects present within each region should be distributed as the χ^2 statistic,

$$\chi^2 = \sum_{i=1}^m (n_i - n_{i,\text{expected}})^2 / n_{i,\text{expected}} \quad (4)$$

where n_i is the observed number of objects in region i and $n_{i,\text{expected}}$ is the mean surface density of objects multiplied by the region’s area. Note that there are no constraints on the size of each region, nor its shape. However, given the limited number of IPN candidates present in our data, we chose to simply divide our CCD fields into rectangles and test for large-scale non-uniformity.

To implement our test, we began by dividing each CCD field into 2×2 , 3×3 , and 4×4 rectangular regions, and calculating the effective area of each region. Note that this second step was not straightforward: bright stars, galaxies, bad pixels, and gaps between the CCDs in our MOSAIC fields (Fields 7 and 8) all act to limit our IPN survey area. To account for these effects, we very carefully masked out all those regions where the IPN detections would be abnormally difficult (or impossible), and restricted our analyses to the areas outside these regions.

Our next step was to choose samples of IPNe for analysis. Our IPN detections on a frame are 90% complete down to a limiting magnitude of m_{lim} ; if we restrict our study to objects brighter than this, then we can be assured that our quadrat analysis will not be biased. However, it is possible (and even likely) that the probability of detecting an IPN below the completeness limit is independent of frame position, and only a function of shot noise. If this is the case, then we can use our entire sample of IPNe (which is typically a factor of ~ 2 larger than the statistically complete sample), and still obtain a result that is bias-free. To test for this possibility, we performed our quadrat analysis on both the statistically complete sample, and on our entire sample of IPN candidates. For Fields 4 and 5 however, there are simply too few objects to measure the spatial distribution for the statistically complete sample.

Tables 1 and 2 contain the results of our analysis. From the table, it is clear that the IPNe in several of our fields are non-randomly distributed. The best evidence for this effect occurs in Field 7, where the statistically complete sample of IPNe are non-randomly distributed at the 95% confidence level, and the entire sample of IPNe are non-random with 99.9% confidence. Fields 2 and 4 also show some evidence for clustering, although the signal is weaker. When their entire IPN samples in these fields are used, random distributions are excluded with 95% confidence.

An examination of Figure 3 reveals that the features found by the quadrat analysis are easily seen by eye. The signal for Field 2 comes from the absence of objects in the lower portion of the frame, while Field 4’s non-random result is generated by the cluster of objects in the upper left-hand corner. Finally, the large χ^2 of Field 7 comes from the east-west division of IPNe and the two large areas where IPN candidates are seen. These non-uniformities range in scale from $1'0$ to $9'0$, and are in agreement with the conclusions of Okamura et al. (2002; see their Figure 1) who find an inhomogeneous distribution of IPNe in their Subaru 1 field.

How do these results compare with the “Harassment” scenarios of Moore et al. (1996)? By both visual inspection of the Moore et al. (1996) simulations, and order-of-magnitude arguments, the width of tidal debris arcs should be ~ 50 kpc, which corresponds to $\sim 12' D_{15}^{-1}$ in the Virgo cluster. Observations of such arcs in the Coma and Centaurus clusters (Trentham & Mobasher 1998; Gregg & West 1998; Calcaño-Roldán, et al. 2000), confirm that tidal tails are often ~ 5 to ~ 40 kpc in width ($1 - 10'0 D_{15}^{-1}$). This implies that a tidal debris arc would fill a significant portion of a PFCCD frame, and up to one one-third of a Mosaic field. Therefore, the non-uniformities detected in our analysis are more likely to indicate small scale inhomogeneities, either within a longer tidal arc, or possibly unrelated to arcs. More wide-field data will be needed to unambiguously search for long thin tidal

debris arcs in the Virgo cluster.

We note that since the density of contaminating sources is approximately 20%, it is unlikely that they could have produced the signal found by our quadrat analysis. The evidence from both Lyman-Break galaxy surveys (Adelberger et al. 1998; Giavalisco & Dickinson 2001), and higher redshift Lyman- α galaxy surveys (Ouchi et al. 2003), suggests that high redshift galaxies cluster on somewhat smaller angular scales ($\approx 2 - 3'$) than seen in our data. Still, the best way to confirm our clustering results is to obtain velocities for the IPN candidates. If these objects are part of a tidal debris arc, or other related structure, they will be strongly correlated in velocity, as well as position. Adding this third dimension is crucial to the interpretation of these data.

4. The Amount of Intracluster Starlight

In principle, determining the amount of intracluster luminosity from the observed numbers of IPNe is straightforward. Theories of simple stellar populations (e.g., Renzini & Buzzoni 1986) have shown that the bolometric luminosity-specific stellar evolutionary flux of non-star-forming stellar populations should be $\sim 2 \times 10^{-11}$ stars-yr $^{-1}$ - L_{\odot}^{-1} , (nearly) independent of population age or initial mass function. If the lifetime of the planetary nebula stage is $\sim 25,000$ yr (Kwok 2000), and if the PNLf of equation (2) is valid to ~ 8 mag below the PNLf cutoff, then every stellar system should have $\alpha \sim 50 \times 10^{-8}$ PN- L_{\odot}^{-1} . According to equation (2), approximately one out of ten of these PNe will be within 2.5 mag of M^* . Thus, under the above assumptions, most stellar populations should have $\alpha_{2.5} \sim 50 \times 10^{-9}$ PN- L_{\odot}^{-1} . The observed number of IPNe, coupled with equation (2), can therefore be used to deduce the total luminosity of the underlying stellar population.

Unfortunately, there are a number of systematic uncertainties associated with this conversion that must be addressed before we can use IPN surface densities to estimate the intracluster luminosity. We discuss each of these uncertainties below and determine a conservative correction for each effect.

4.1. Systematic Uncertainties

Although stellar evolution predicts a constant $\alpha_{2.5}$ value for all non star-forming populations, observations present a more complicated picture. Ciardullo (1995) found that in a sample of 23 elliptical galaxies, lenticular galaxies, and spiral bulges, the observed value of $\alpha_{2.5}$ never exceeded $\alpha_{2.5} = 50 \times 10^{-9}$ PN- L_{\odot}^{-1} but was often significantly less, with

higher luminosity galaxies having systematically smaller values of $\alpha_{2.5}$, down to values of $\alpha_{2.5} = 8.3 \pm 1.5 \times 10^{-9}$ for M87 and $\alpha_{2.5} = 6.5 \pm 1.4 \times 10^{-9}$ for M49. A lower value for $\alpha_{2.5}$ has also been inferred for the populations of Galactic globular clusters ($\alpha_{2.5} \approx 13$; Jacoby et al. 1997). The reason for this discrepancy is unclear. It is possible that in old or metal-rich populations, not all stars go through the planetary nebula phase (Ciardullo 1995; Jacoby et al. 1997); such an hypothesis is supported by the anti-correlation between $\alpha_{2.5}$ and the presence of extreme horizontal branch stars in elliptical galaxies (Ferguson 1999). Alternatively, the PNLf may not always follow the simple exponential law of equation (2). Ciardullo et al. (2004) have recently shown that in star-forming populations, the PNLf has a distinctive ‘dip’ ~ 2 mag below the PNLf cutoff; if similar features occur in older populations, then the extrapolation to the faint end of the luminosity function may be inaccurate. In either case, since the total amount of intracluster luminosity depends on $\alpha_{2.5}$, the variation of $\alpha_{2.5}$ with stellar population can be a significant source of error, especially considering that our constraints on the age and metallicity of the stellar population are still weak (Paper I; Durrell et al. 2002).

To correct for this effect, we adopted the results of Durrell et al. (2002), who used the *Hubble Space Telescope* to measure the luminosity function of red giants in Virgo’s intracluster space. Models demonstrate that these data can be easily scaled to give the total luminosity of the intracluster population in this field (e.g., Girardi et al. 2000). By comparing the numbers of IPNe in Field 7, which surrounds the *HST* field, with RGB and AGB star counts, Durrell et al. (2002) found a value of $\alpha_{2.5} = 23_{-12}^{+10} \times 10^{-9} \text{ PN-}L_{\odot}^{-1}$ for Virgo’s intracluster population. This value is similar to that derived for the bulges of spiral galaxies, and we adopt it here for our luminosity calculations. However, even this determination has a substantial systematic uncertainty. As we have noted in §3.2, the intracluster stars are not uniformly distributed on the sky, and the *HST* survey field is only $\sim 1/20$ the size of Field 7. Thus there is the possibility of a density mismatch between the two measurements due to the spatial structure of the intracluster light. At this time, we cannot determine the amount of this effect: additional intracluster red giant fields will be needed for a more accurate comparison.

A second systematic error associated with our measurements comes from the fact that samples of IPN candidates are not pristine. Approximately 20% of our IPN candidates are background objects of various kinds, of which the most common are Lyman- α galaxies at $z \approx 3.12$ (e.g., Kudritzki et al. 2000; Rhoads et al. 2000; Stern et al. 2000). The only absolutely secure way to eliminate these contaminants is through spectroscopy: true IPNe have narrow ($\sim 30 \text{ km s}^{-1}$) emission lines, show additional flux at [O III] $\lambda 4959$, and have an [O III] $\lambda 5007$ to H α emission line ratio of $\gtrsim 2$ (Ciardullo et al. 2002b). This distinguishes IPNe from background galaxies (which have broader lines and no companion emission) or

intergalactic H II regions (which usually have an H α line that is brighter than [O III] λ 5007). Unfortunately, since we do not yet have follow-up spectroscopy for our IPN candidates, we must statistically remove the background contaminants using the methods detailed in Paper II and in Ciardullo et al. (2002a). Using a set of control fields, and identical search procedures as the Virgo IPN survey, we determined the surface density of IPN-like objects, and adopted that density as our mean background (69 ± 23 per square degree brighter than $m_{5007} = 27.0$). This density is corrected in each field for any known background objects (Paper II).

There are a number of complications to this background subtraction. First, as noted in Paper II, the Ciardullo et al. (2002a) survey only covered 0.13 deg^{-2} of sky, and thus detected only nine unresolved IPNe-like objects. Consequently, the estimate of background density has a large Poissonian error. Of greater concern is the effect that cosmic large-scale structure has on the background source counts. Recent observations by Ouchi et al. (2003) find that Lyman- α galaxies are already clustered at $z=4.86$, which implies even greater clustering at $z \approx 3$. Combined with the $z \approx 3$ Lyman-break galaxy results of Adelberger et al. (1998) and Giavalisco & Dickinson (2001), it is almost certain that our background estimation is affected by the large-scale structure exhibited by emission-line galaxies. We do note that our contamination fraction is similar to the $\sim 26\%$ value found by Freeman et al. (2000) from limited follow-up spectroscopy and the $\sim 15\%$ estimate of Castro-Rodríguez et al. (2003) based on a narrow-band survey of a field in the Leo I galaxy group. Ultimately additional blank field measurements and spectroscopic follow-ups will be needed to further reduce the uncertainty.

Finally, as noted in §3.2, the IPN candidates of Virgo have a significant line-of-sight depth. Because our observations do not reach all the way through the cluster, our density determination is biased: we are more likely to detect IPNe on the near side of the cluster than the far side. In Paper I, we created two extreme models for the IPN distribution: a minimal ICL model, wherein all the IPNe are at a single distance, and a maximum ICL model, in which the intracluster stars are distributed isotropically throughout a sphere of radius 3 Mpc. The difference in densities between these two models is a factor of ~ 3 . Therefore, we are faced with a quandary: do we assume a spherically symmetric model, and multiply the measured densities by a factor of three, or do we adopt the single distance model that we know to be incorrect? In order to be conservative, we have chosen the latter option, and adopt a single distance model for all of our intracluster fields. In the future, when our studies of the line-of-sight densities are completed, we will be able to obtain a more accurate answer.

In conclusion, although there are significant systematic uncertainties relating the number

of IPNe to the total amount of starlight, we believe we have reasonable corrections to these effects which are conservative, and supported by the data.

4.2. Fitting the PNLFs, and Determining the Amount of Intracluster Light

To determine the amount of luminosity in each of our survey fields, we began by adopting the PNLf of equation (2), and convolving it with the photometric error versus magnitude relation derived from our photometry. We then computed the likelihood of this model luminosity function fitting the observed statistical sample of PNe as a function of two variables, system distance and total PN population (Ciardullo et al. 1989). We then integrated over the former variable, reduced the latter variable by the fraction of contamination expected for each field, and then translated the PN populations into intracluster luminosity via our best-fit value for $\alpha_{2.5}$. These results appear in Table 3, column 2. The quoted errors are the formal uncertainties associated with the maximum likelihood solutions; these are usually asymmetric due to the shape of the [O III] $\lambda 5007$ planetary nebulae luminosity function. In the case of Field 3, we have shown previously that the PNe in this field are a combination of IPNe, and PNe in the halo of M 87 proper, and that at least 10 of these objects can legitimately be called IPNe (Paper I). Therefore, to place limits on this field’s intracluster light, we assumed that 1) all of the PNe candidates in this field are intracluster, or 2) that only the brightest 10 candidates are intracluster. These two models are referred to as “3h” and “3l” respectively. For Fields 4 and 5, due to the very small number of objects above the completeness limit, the uncertainties are poorly constrained. In these cases, we replaced the maximum-likelihood error bars with the errors expected from Poissonian statistics. For Field 8, the IPN density is consistent with zero, so no analysis has been performed in this region.

As expected, the amount of intracluster light is significant: the intracluster luminosity contained within our average PFCCD survey field is comparable to that of the Large Magellanic Cloud. The implied bolometric luminosity surface densities, denoted as Σ_{IPN} , are given in Table 3, column 3. For reference, these densities are roughly ~ 40 times less than that of the Milky Way’s disk at the solar neighborhood (de Vaucouleurs & Pence 1978). If we adopt a bolometric correction consistent with a late-type stellar population, (-0.80), these bolometric luminosity surface densities can be translated into V -band surface brightnesses. These are given in Table 3, column 4. Although the surface brightnesses are quite faint (5–6 magnitudes below that of the night sky), they are reachable with the newer generation of CCD ICL surveys now being performed, provided that precise and accurate sky subtraction can be achieved (Gonzalez et al. 2000; Feldmeier et al. 2002; Krick & Bernstein 2003; Mihos

et al. 2004, in prep.).

With the luminosity of Virgo’s intracluster stars now determined, we can next compare this number to the amount of light contained within the cluster’s galaxies. This is non-trivial, because as we mentioned previously, the structure of Virgo is unrelaxed, and difficult to model accurately.

To estimate this quantity, we used the galaxy catalog of Binggeli, Sandage, & Tammann (1985) to find the total B -band magnitudes of all member galaxies brighter than the catalog’s limit of $B_T \sim 20$. (This limit is adequate for our purpose, since the contribution of fainter objects to Virgo’s total luminosity is negligible.) We then converted these B -magnitudes to I , using the observed $B - I$ colors of early-type galaxies (Goudfrooij et al. 1994) and a mean $(B - I)$ color for late-type galaxies (de Jong & van der Kruit 1994). Finally, with the I magnitudes of all the galaxies in hand, we computed the radial profile of Virgo in bolometric light, using an I -band bolometric correction of +0.4. Note that to do this, we must determine the center of the cluster. Binggeli, Tammann & Sandage (1987) have shown that the luminosity density of Virgo peaks $\sim 58'$ NW of the central elliptical, M87. However, based on the cluster’s kinematics (Binggeli, Popescu, & Tammann 1993), distances (Jacoby, Ciardullo, & Ford 1990; Tonry et al. 2001; West & Blakeslee 2000; Ferrarese et al. 2000), and X-ray properties (Bohringer et al. 1994; Schindler, Binggeli, & Böhringer 1999), it is likely that this offset is due to the contribution of the M84/M86 Group, which is falling into Virgo from behind. We therefore used M87 as the central point, and computed the I -band luminosity density of Virgo’s galaxies in a series of circular apertures centered on the galaxy.

The luminosity surface densities we derive are given in Table 3, column 5, which we denote as Σ_{galaxies} . For Fields 2 and 6, which are in subcluster B of Virgo, the circular aperture model derived above is not applicable, since that subcluster has an irregular galaxy distribution. Therefore, to set a robust lower limit on the fraction derived for Fields 2 and 6, we assumed a value for Σ_{galaxies} that is representative of the center of subcluster A.

Finally, we computed the fraction of intracluster light in each field by dividing Σ_{IPN} by the sum of Σ_{galaxies} and Σ_{IPN} . At this point, to make error analysis more tractable, we also adopted the average uncertainty of our asymmetric density error bars. Based on all of these assumptions, we derive intracluster star fractions between 4% and 41%, depending on the field. When averaged over all our fields, the fraction of intracluster light in Virgo is $18.5\% \pm 3.0\%$ (excluding Field 8) and $15.8\% \pm 3.0\%$ (with Field 8 included). The quoted uncertainties include only the random component; the systematic uncertainties are dominated by the uncertain line-of-sight depth of the intracluster stars, and the error associated with our estimate of $\alpha_{2.5}$. We estimate that these systematic errors could be as large as 5%. However, by assuming a single-limit distance for the intracluster starlight, we have underestimated the

total amount of intracluster light, and therefore the fractions quoted above are conservative.

To ensure that our values for Σ_{galaxies} are reasonable, we have also calculated local luminosity surface densities for each field to compare against our IPN luminosity densities. To do this, we defined two densities, Σ_{25} and Σ_{50} , to be the amount of bolometric luminosity density associated with the 25 and 50 Binggeli, Sandage, & Tammann (1985) galaxies closest to the center of each of our survey fields, omitting clear background galaxies. We then used these densities to normalize our IPN measurements in exactly the same way as described above. The results are given in Table 4. For any individual field, there can be a large difference between the locally and globally derived luminosity fractions. This is expected, given the clumpy, unrelaxed state of the cluster, and the limited number of luminous galaxies near each field. However, the weighted mean of these two local determinations for the entire cluster is $15.7\% \pm 1.4\%$ (including Field 8), essentially identical to our previous result.

These fractions agree with single field studies of Virgo’s intracluster population. Arnaboldi et al. (2002) found a fraction of at least 17% from the observations of field RCN1, and Okamura et al. (2002), and Arnaboldi et al. (2003) estimated a fraction of 10% from IPN data of the Subaru 1 field. Similarly, Ferguson, Tanvir & von Hippel (1998) found fractions of between 4% and 12% using *HST* observations of IRG’s, and Durrell et al. (2002) obtained a fraction of $15^{+7}_{-5}\%$ using the red giant measurements of two *HST* fields. However, it is important to note that each of these studies makes different assumptions concerning the calculation of intracluster luminosity, the amount of light bound to galaxies, and the contamination of background sources. So none of these numbers is unassailable.

How much stellar mass does this amount of intracluster light imply? If we take our value for the median luminosity surface density of intracluster light ($6.4 \times 10^5 L_{\odot} \text{ kpc}^{-2}$), and assume a bolometric correction of -0.80 (a value typical of older stellar populations) and a mass-to-light ratio of $M/L_V \sim 7.7$ (Buzzoni 1989), then the derived surface mass density of Virgo’s intracluster stars is $7.3 \times 10^{11} M_{\odot} \text{ Mpc}^{-2} D_{15}^{-2}$. Although this mass density seems large, when compared to a detailed mass model of the three Virgo subclusters (Schindler, Binggeli, & Böhringer 1999; Schindler 2002), and after correcting for the different assumed distances to the Virgo core in the two calculations (15 Mpc versus 20 Mpc), we find that the intracluster stars add on average of $\approx 17\%$ to the stellar mass of the cluster. In any case, as in most galaxy clusters, the majority of the baryonic mass of Virgo is in the intracluster gas (Schindler, Binggeli, & Böhringer 1999; Schindler 2002), and the baryonic mass itself is only a fraction of the total mass. Intracluster stars do not solve the missing-mass problem in galaxy clusters, as was originally determined by de Vaucouleurs (1960).

The radial distribution of the IPNe compared to that of the cluster light is shown in Figure 4. As can be clearly seen, the IPN density falls slowly, if it all, and certainly more

slowly than that of the galaxies. If we fit the IPN densities with a simple power law in radius we find that the least-squares slope is -0.1 ± 0.5 . Given the uncertainties associated with the measurements, this result is marginally consistent with the simulations of Dubinski (1998), and Napolitano (2003), which predict $r^{1/4}$ like profiles for the intracluster light.

Since galaxy morphology correlates strongly with galactic density (Dressler 1980), it is conceivable that IPNe density also correlates with this quantity. To test this hypothesis, we obtained the local projected galaxy density for each field by taking the catalog of Binggeli, Sandage, & Tammann (1985), and finding all Virgo galaxies within $100D_{15}$ kpc in radius ($23'3''$) of each field center. By using this catalog, we are sensitive to objects at least as faint as $M_B \sim -13$, and in some cases, two magnitudes fainter, which puts our density measurement into the domain of intermediate dwarf galaxies. This number density, denoted as N_{100} , is given in Table 3, column 7, and plotted against the IPN density in Figure 5.

As can be clearly seen, there appears to be little or no correlation between intracluster light density and projected galaxy density. After fitting the data to a simple power-law, we find a slope of -0.1 ± 0.4 in units of $\log \Sigma / \log N_{100}$. This null result is somewhat surprising, since if intracluster light is produced from galaxy interactions, a correlation with density might be expected. We repeated this test over radii of 200, 500, and $1000D_{15}$ kpc respectively, and found similar null results (no positive slope at greater than the 2σ level).

These null results may be due to the significant scatter in the projected density, as well as the known uncertainties in the intracluster stellar densities. Alternatively, the dynamic range of density surveyed in this analysis may be too small (a factor of ~ 2) compared to that needed to see the morphology-density relation. Finally, our measurements may suffer from an unavoidable selection effect. In order to avoid confusion with PNe which are bound in the halos of galaxies, we must conduct our intracluster light survey in regions where there are no bright objects. In the past, these locations may have been occupied by bright galaxies, and the intracluster stars may have been released from these objects. However, given the large amount of time that could have elapsed between the release of these stars and the present epoch, it is possible that the IPNe have drifted more than the adopted $100\text{--}1000D_{15}$ kpc radii. More intracluster observations over a larger range of cluster densities will be needed to address this issue further.

5. Discussion

When we combine our own IPN data, the results from intracluster red giant observations (Ferguson, Tanvir, & von Hippel 1998; Durrell et al. 2002), and other IPN surveys (Arnaboldi

et al. 1996, 2002; Okamura et al. 2002; Arnaboldi et al. 2003), we come to a reasonably consistent picture of Virgo’s stellar intracluster population.

There is a moderate (10–20%) amount of intracluster light in the Virgo cluster, significantly more than found in the galaxy groups of M 81 ($< 3\%$; Feldmeier et al. 2003b) and Leo I ($1.6^{+3.4}_{-1.0}\%$; Castro-Rodríguez et al. 2003), but much less than is present in the rich clusters of Coma ($\sim 50\%$; Bernstein et al. 1995), Abell 1689 ($\approx 30\%$; Tyson & Fischer 1995), and the compact group HCG 90 (38%–48%; White et al. 2003). This is consistent with the view that Virgo is a dynamically young cluster still in the process of formation (Tully & Shaya 1984; Binggeli, Tammann & Sandage 1987; Binggeli, Popescu, & Tammann 1993). As Virgo dynamically evolves, the amount of intracluster light should increase.

From the large depth derived from the IPNe, it seems clear that a significant portion of Virgo’s intracluster stars originate from late-type galaxies whose highly radial orbits take them in and out of the cluster core. The intermediate value of $\alpha_{2.5}$ also strongly implies that the bulk of the IPNe come from lower-luminosity galaxies, and not giant ellipticals ($M_B \geq -20$; Ciardullo 1995). This conclusion is supported by the intracluster red giant star observations of Durrell et al. (2002). Their analysis of the intracluster red giant luminosity function shows that Virgo’s intracluster stars have a mean metallicity in the range $-0.8 < [\text{Fe}/\text{H}] < -0.2$. Such a value is more metal-rich than a typical dwarf galaxy (Shetrone, Côté, & Sargent 2001), yet more metal-poor than the giant ellipticals that inhabit the Virgo cluster core (i.e., Terlevich et al. 1981; Davies et al. 1987). Moreover, the value of $\alpha_{2.5}$ derived for the IPN population, and the IPN properties described in Ciardullo et al. (1998) and Paper I suggest that the intracluster stars of Virgo are not extremely old or young. If the IPN were extremely old, then the depth of the Virgo cluster would be even higher than its large derived value (Paper I), and measurements of $\alpha_{2.5}$ in young stellar populations such as the Magellanic Clouds give values near the theoretical maximum (Ciardullo et al. 1995). These facts, along with the lack of correlation between IPN density and galactic environment, imply that the production of intracluster stars is an ongoing process.

The above properties appear consistent with tidal-stripping from galaxy interaction (Richstone & Malumuth 1983) scenarios such as “galaxy harassment” (Moore et al. 1996; Moore, Lake, & Katz 1998) “tidal stirring” (Mayer et al. 2001), and “galaxy threshing” (Bekki et al. 2003) and are inconsistent with tidal stripping by the mean cluster field very early in the cluster’s lifetime (Merritt 1984). However, a few caveats are in order. First, since we derive properties through the IPNe, any stellar population that is extremely old and metal-poor (Jacoby et al. 1997), or very metal-rich (Ciardullo 1995), will not produce large numbers of IPNe, and so will be missed in our survey. If there was a large amount of intracluster star production at early times, it would be extremely old, and we would be

insensitive to this population. The close agreement between the IRG and the IPN observations makes the existence of a large Pop II/III component unlikely, but some extremely old intracluster stars may still exist. Also, since IPNe are weighted by stellar luminosity, the properties of rarer populations, such as those produced by tidally-stripped dwarf galaxies, will be poorly represented in our survey. It is almost certain that some of Virgo’s intracluster light originated from fainter dwarfs that have undergone severe tidal disruption and now exist as a population of Ultra-Compact Dwarf galaxies (Drinkwater et al. 2003; Karick et al. 2003).

There are a number of further studies that can improve the results given in this paper. Additional IPN fields, especially ones at larger cluster radii and at lower galaxy densities, would be invaluable in confirming our null results with respect to galaxy density and radial distribution. Deep imaging of a single field would also assist in better defining the line-of-sight distribution of IPNe. But the most important observations needed are follow-up spectroscopy for a large number of candidate IPNe. Such observations would remove the uncertainty in our results due to background sources, produce better IPN magnitudes, and most critically, allow comparison of Virgo’s intracluster population with dynamical models.

We thank M. Arnaboldi, K. Freeman, R. Kudritzki, R. Méndez, and Chris Mihos for useful discussions, and their infinite patience. We also thank an anonymous referee for their comments which improved this paper. J. Feldmeier acknowledges salary support from J.C. Mihos under grant AST-9876143. This work was also partially supported by NSF grant AST 0071238, AST 0302030, and NASA grant NAG 5-9377.

REFERENCES

- Abell, G. O. 1961, *AJ*, 66, 607
- Adelberger, K. L., Steidel, C. C., Giavalisco, M., Dickinson, M., Pettini, M., & Kellogg, M. 1998, *ApJ*, 505, 18
- Arnaboldi, M., et al. 1996, *ApJ*, 472, 145
- Arnaboldi, M., et al. 2002, *AJ*, 123, 760
- Arnaboldi, M., et al. 2003, *AJ*, 125, 514
- Bekki, K., Couch, W. J., Drinkwater, M. J., & Shioya, Y. 2003, *MNRAS*, 344, 399
- Bernstein, G. M., Nichol, R. C., Tyson, J. A., Ulmer, M. P., & Wittman, D. 1995, *AJ*, 110, 1507
- Binggeli, B., Popescu, C. C., & Tammann, G. A. 1993, *A&AS*, 98, 275
- Binggeli, B., Sandage, A., & Tammann, G.A. 1985, *AJ*, 90, 1681
- Binggeli, B., Tammann, G. A. & Sandage, A. 1987, *AJ*, 94, 251
- Bohringer, H., Briel, U. G., Schwarz, R. A., Voges, W., Hartner, G., & Trumper, J. 1994, *Nature*, 368, 828
- Bolte, M. 1989, *ApJ*, 341, 168
- Buzzoni, A. 1989, *ApJS*, 71, 817
- Calcáneo-Roldán, C. , Moore, B. , Bland-Hawthorn, J. , Malin, D., & Sadler, E. M. 2000, *MNRAS*, 314, 324
- Castro-Rodríguez, N., Aguerri, J. A. L., Arnaboldi, M., Gerhard, O., Freeman, K. C., Napolitano, N. R., & Capaccioli, M. 2003, *A&A*, 405, 803
- Ciardullo, R. 1995, in *IAU Highlights of Astronomy*, 10, ed. I. Appenzeller (Dordrecht: Kluwer), p. 507
- Ciardullo, R., Durrell, P. R., Laychak, M. B., Herrmann, K. A., Moody, K., Jacoby, G. H., & Feldmeier, J. J., 2004, *ApJ*, in press
- Ciardullo, R., Jacoby, G. H., Feldmeier, J. J., & Bartlett, R. E. 1998, *ApJ*, 492, 62

- Ciardullo, R., Feldmeier, J. J., Krelove, K., Jacoby, G. H., & Gronwall, C. 2002a, *ApJ*, 566, 784
- Ciardullo, R., Feldmeier, J. J., Jacoby, G. H., Kuzio, R., Laychak, M. B., & Durrell, P. R. 2002b, *ApJ*, 577, 31
- Ciardullo, R., Jacoby, G. H., & Ford, H. C. 1989, *ApJ*, 344, 715
- Ciardullo, R., Jacoby, G. H., Ford, H. C., & Neill, J. D. 1989, *ApJ*, 339, 53
- Davies, R. L., Burstein, D., Dressler, A., Faber, S. M., Lynden-Bell, D., Terlevich, R. J., & Wegner, G. 1987, *ApJS*, 64, 581
- de Jong, R.S., & van der Kruit, P.C. 1994, *A&AS*, 106, 451
- de Vaucouleurs, G. 1960, *ApJ*, 131, 585
- de Vaucouleurs, G. & de Vaucouleurs, A. 1973, *A&A*, 28, 109
- de Vaucouleurs, G. & Pence, W. D. 1978, *AJ*, 83, 1163
- Diggle, P. J. 1983, *Statistical Analysis of Spatial Point Patterns* (Academic Press)
- Dopita, M. A., Jacoby, G. H., & Vassiliadis, E. 1992, *ApJ*, 389, 27
- Dressler, A. 1980, *ApJ*, 236, 351
- Drinkwater, M.J., Gregg, M.D., & Colless, M. 2001, *ApJ*, 548, L139
- Drinkwater, M. J., Gregg, M. D., Hilker, M., Bekki, K., Couch, W. J., Ferguson, H. C., Jones, J. B., & Phillipps, S. 2003, *Nature*, 423, 519
- Dubinski, J. 1998, *ApJ*, 502, 141
- Dubinski, J., Murali, C., & Ouyed, R. 2000, unpublished preprint
- Durrell, P. R., Ciardullo, R., Feldmeier, J. J., Jacoby, G. H., & Sigurdsson, S. 2002, *ApJ*, 570, 119
- Federspiel, M., Tammann, G. A., & Sandage, A. 1998, *ApJ*, 495, 115
- Feldmeier, J. J. 2000, Ph.D. Thesis, Penn State University
- Feldmeier, J. J. 2003, in *IAU Symp. 209, Planetary Nebula: Their Evolution and Role in the Universe*, ed. S. Kwok, M. Dopita, & R. Sutherland (San Francisco: ASP), 597

- Feldmeier, J. J., Ciardullo, R., & Jacoby, G. H. 1998 (Paper I), *ApJ*, 503, 109
- Feldmeier, J. J., Ciardullo, R., Jacoby, G. H., & Durrell, P.R. 2003a, (Paper II) *ApJS*, 145, 65
- Feldmeier, J.J., Durrell, P.R., Ciardullo, R., & Jacoby, G.H. 2003b, in IAU Symposium No. 209 Planetary Nebulae: Their Evolution and Role in the Universe, ed. S. Kwok, M. Dopita, & R. Sutherland (San Francisco: ASP), 605
- Feldmeier, J. J., Mihos, J. C. M., Morrison, H. L., Rodney, S. A., & Harding, P. 2002, *ApJ*, 575, 779
- Ferguson, H. C. 1999, *Ap&SS*, 267, 263
- Ferguson, H. C., Tanvir, N. R., & von Hippel, T. 1998, *Nature*, 391, 461
- Ferrarese, L., et al. 2000, *ApJ*, 529, 745
- Freedman, W. L., et al. 2001, *ApJ*, 553, 47
- Freeman, K. C. et al. 2000, ASP Conf. Ser. 197: Dynamics of Galaxies: from the Early Universe to the Present, ed. F. Combes, G. A. Mamon, & V. Charmandaris (San Francisco: ASP), 389.
- Gal-Yam, A., Maoz, D., Guhathakurta, P., & Filippenko, A. V. 2003, *AJ*, 125, 1087
- Gallagher, J. S., & Ostriker, J. P. 1972, *AJ*, 77, 288
- Gerhard, O., Arnaboldi, M., Freeman, K. C., & Okamura, S. 2002, *ApJ*, 580, L121
- Giavalisco, M. & Dickinson, M. 2001, *ApJ*, 550, 177
- Girardi, L., Bressan, A., Bertelli, G., & Chiosi, C. 2000, *A&AS*, 141, 371
- Gonzalez, A. H., Zabludoff, A. I., Zaritsky, D., & Dalcanton, J. J. 2000, *ApJ*, 536, 561
- Goudfrooij, P., Hansen, L., Jorgensen, H.E., Norgaard-Nielsen, H.U., de Jong, T., & van den Hoek, L.B. 1994, *A&AS*, 104, 179
- Gregg, M. D., & West, M. J. 1998, *Nature*, 396, 549
- Gunn, J. E. & Gott, J. R. I. 1972, *ApJ*, 176, 1
- Harris, W. E. 1990, *PASP*, 102, 949

- Jacoby, G. H. 1989, *ApJ*, 339, 39
- Jacoby, G. H., et al. 1992, *PASP*, 104, 599
- Jacoby, G. H., Ciardullo, R., & Ford, H. C. 1990, *ApJ*, 356, 332
- Jacoby, G. H., Morse, J. A., Fullton, L. K., Kwitter, K. B., & Henry, R. B. C. 1997, *AJ*, 114, 2611
- Jerjen, H., Binggeli, B. & Barazza, F.D. 2004, *AJ*, 127, 771
- Jordán, A., West, M. J., Côté, P., & Marzke, R. O. 2003, *AJ*, 125, 1642
- Karick, A.M., Drinkwater, M.J., West, M., Gregg, M.D., Hilker, M. 2003, in *IAU Symposium 217, Recycling Intergalactic and Interstellar Matter*, ASP Conf. Series, astro-ph/0310448
- Krick, J. E., & Bernstein, R. 2003, in *Carnegie Observatories Astrophysics Series, Vol. 3: Clusters of Galaxies: Probes of Cosmological Structure and Galaxy Evolution*, ed. J. S. Mulchaey, A. Dressler, and A. Oemler (Pasadena: Carnegie Observatories)
- Kudritzki, R.-P., Méndez, R. H., Feldmeier, J. J., Ciardullo, R., Jacoby, G. H., Freeman, K.C., Arnaboldi, M., Capaccioli, M., Gerhard, O., & Ford, H.C. 2000, *ApJ*, 536, 19
- Kwok, S. 2000, in *The Origin and Evolution of Planetary Nebulae*, p. 118 (New York: Cambridge)
- Mamon, G. A., Sanchis, T., Salvador-Solé, E., & Solanes, J. M. 2004, *A&A*, 414, 445
- Massey, P., Strobel, K., Barnes, J. V., & Anderson, E. 1988, *ApJ*, 328, 315
- Mayer, L., Governato, F., Colpi, M., Moore, B., Quinn, T., Wadsley, J., Stadel, J., & Lake, G. 2001, *ApJ*, 547, L123
- Melnick, J., White, S. D. M., & Hoessel, J. 1977, *MNRAS*, 180, 207
- Méndez, R. H. & Soffner, T. 1997, *A&A*, 321, 898
- Merritt, D. 1983, *ApJ*, 264, 24
- Merritt, D. 1984, *ApJ*, 276, 26
- Mihos, J. C. 2004a, in *IAU Symposium 217, Recycling Intergalactic and Interstellar Matter*, available as astro-ph/0401557

- Mihos, J. C., et al. 2004, ApJ, in preparation
- Miller, G. E. 1983, ApJ, 268, 495
- Mohr, J. J., Evrard, A. E., Fabricant, D. G., & Geller, M. J. 1995, ApJ, 447, 8
- Monet, D. 1998, BAAS, 30, 1427
- Monet, D., et al. 1996, USNO A - 1.0 a catalog of astrometric standards, U.S. Naval Observatory, Washington, D. C.
- Moore, B., Diemand, J., & Stadel, J. in Outskirts of Galaxy Clusters: intense life in the suburbs ed. A. Diaferio, IAU Colloquium N. 195., available as astro-ph/0406615
- Moore, B., Katz, N., Lake, G., Dressler, A., & Oemler, A. 1996, Nature, 379, 613
- Moore, B., Lake, G. & Katz, N. 1998, ApJ, 495, 139
- Muccione, V. & Ciotti, L. 2004, A&A, 421, 583
- Muller, G. P., Reed, R., Armandroff, T., Boroson, T. A., & Jacoby, G. H. 1998, Proc. SPIE, 3355, 577
- Napolitano, N. R., et al. 2003, ApJ, 594, 172
- Neilsen, E. H. & Tsvetanov, Z. I. 2000, ApJ, 536, 255
- Okamura, S., et al. 2002, PASJ, 54, 883
- Ouchi, M., et al. 2003, ApJ, 582, 60
- Peebles, P. J. E. 1980, The Large-Scale Structure of the Universe (Princeton: Princeton University Press)
- Pierce, M. J., Welch, D. L., McClure, R. D., van den Bergh, S., Racine, R., & Stetson, P. B. 1994, Nature, 371, 385
- Renzini, A., & Buzzoni, A. 1986, in Spectral Evolution of Galaxies, ed. C. Chiosi, & A. Renzini (Dordrecht: Reidel), p. 195
- Rhoads, J. E., Malhotra, S., Dey, A., Stern, D., Spinrad, H., & Jannuzi, B. T. 2000, ApJ, 545, L85
- Richstone D. O., & Malumuth, E. M. 1983, ApJ, 268, 30

- Ryan-Weber, E. V., et al. 2004, *AJ*, 127, 1431
- Saha, A., Sandage, A., Labhardt, L., Tammann, G. A., Macchetto, F. D., & Panagia, N. 1997, *ApJ*, 486, 1
- Sanchis, T., Solanes, J. M., Salvador-Solé, E., Fouqué, P., & Manrique, A. 2002, *ApJ*, 580, 164
- Schindler, S. 2002, in Ringberg Workshop on the Virgo Cluster, astro-ph0206272
- Schindler, S., Binggeli, B., & Böhringer, H. 1999, *A&A*, 343, 420
- Shapley, H., & Ames, A. 1926, Harvard Circ. No. 294
- Shetrone, M. D., Côté, P., & Sargent, W. L. W. 2001, *ApJ*, 548, 592
- Shibata, R., Matsushita, K., Yamasaki, N. Y., Ohashi, T., Ishida, M., Kikuchi, K., Böhringer, H., & Matsumoto, H. 2001, *ApJ*, 549, 228
- Solanes, J. M., Sanchis, T., Salvador-Solé, E., Giovanelli, R., & Haynes, M. P. 2002, *AJ*, 124, 2440
- Stanghellini, L. 1995, *ApJ*, 452, 515
- Stern, D., Bunker, A., Spinrad, H., & Dey, A. 2000, *ApJ*, 537, 73
- Stetson, P. B. 1987, *PASP*, 99, 191
- Stetson, P. B., & Harris, W. E. 1988, *AJ*, 96, 909
- Stone, R. P. S. 1977, *ApJ*, 218, 767
- Terlevich, R., Davies, R. L., Faber, S. M., & Burstein, D. 1981, *MNRAS*, 196, 381
- Tonry, J.L., Dressler, A., Blakeslee, J. P., Ajhar, E. A., Fletcher, A. B., Luppino, G. A., Metzger, M. R., & Moore, C.B. 2001, *ApJ*, 546, 681
- Trentham, N. & Mobasher, B. 1998, *MNRAS*, 293, 53
- Tully, R. B. & Shaya, E. J. 1984, *ApJ*, 281, 31
- Tyson, J. A. & Fischer, P. 1995, *ApJ*, 446, L55
- Tyson, J. A., Kochanski, G. P. & dell’Antonio, I. P. 1998, *ApJ*, 498, L107
- Uson, J. M., Boughn, S. P., & Kuhn, J. R. 1991, *ApJ*, 369, 46

- Vílchez-Gómez, R. 1999, ASP Conf. Ser. 170: The Low Surface Brightness Universe, 349
- Víchez-Gomez, R., Pelló, R. & Sanahuja, B. 1994, A&A, 283, 37
- Vollmer, B. & Huchtmeier, W. 2003, A&A, 406, 427
- Welch, G. A., & Sastry G. N. 1971, ApJ, 169, L3
- West, M. J., & Blakeslee, J. P. 2000, ApJ, 543, L27
- West, M. J., Cote, P., Jones, C., Forman, W., & Marzke, R. O. 1995, ApJ, 453, L77
- White, P. M., Bothun, G., Guerrero, M. A., West, M. J., & Barkhouse, W. A. 2003, ApJ, 585, 739
- Willman, B., Governato, F., Mayer, L. & Quinn, T. 2004, MNRAS, submitted, available as astro-ph/0405094
- Yasuda, N., Fukugita, M., & Okamura, S. 1997, ApJS, 108, 417
- Zwicky, F. 1951, PASP, 63, 61

Table 1. Quadrat Analysis of Total Sample

Field	Binning	χ^2	dof	Null Hypothesis Probability
2	2	7.48	3	0.06
2	3	10.9	8	0.21
2	4	26.3	15	0.04
3	2	5.03	3	0.17
3	3	10.4	8	0.24
3	4	11.2	15	0.74
4	2	2.73	3	0.43
4	3	14.2	7	0.05
4	4	20.2	15	0.17
5	2	3.91	3	0.27
5	3	1.98	8	0.98
5	4	9.19	15	0.87
6	2	4.08	3	0.25
6	3	6.51	8	0.59
6	4	12.1	15	0.67
7	2	2.91	3	0.41
7	3	14.9	8	0.06
7	4	44.3	15	< 0.001
8	2	4.07	3	0.25
8	3	5.69	8	0.68
8	4	15.8	15	0.39

Table 2. Quadrat Analysis of Photometrically Complete Sample

Field	Binning	χ^2	dof	Null Hypothesis
				Probability
2	2	3.88	3	0.28
2	3	5.96	8	0.65
2	4	21.3	15	0.13
3	2	6.34	3	0.10
3	3	12.3	8	0.14
3	4	14.2	15	0.51
6	2	5.71	3	0.13
6	3	6.02	8	0.65
6	4	14.1	15	0.52
7	2	1.29	3	0.73
7	3	7.24	8	0.51
7	4	25.2	15	0.05
8	2	6.16	3	0.10
8	3	10.4	8	0.24
8	4	17.3	15	0.30

Table 3. Luminosity Results - Global Density

Field	Luminosity ($10^9 L_{\odot}$)	Σ_{IPN} ($10^5 L_{\odot} \text{ kpc}^{-2}$)	Surface Brightness ($\mu_{\text{V}} \text{ mag arcsec}^{-2}$)	Σ_{galaxies} ($10^5 L_{\odot} \text{ kpc}^{-2}$)	Fraction ($\Sigma_{\text{IPN}} / \Sigma_{\text{galaxies}} + \Sigma_{\text{IPN}}$)
2	$3.9^{+1.7}_{-3.3}$	8.4	27.4	15.2	0.35 ± 0.22
3h	$9.0^{+1.2}_{-1.4}$	19.9	26.5	107	0.16 ± 0.02
3l	$2.0^{+0.6}_{-0.8}$	4.5	28.1	107	0.04 ± 0.01
4	$2.4^{+1.7}_{-1.7}$	8.3	27.4	13.5	0.37 ± 0.26
5	$3.5^{+2.0}_{-2.0}$	9.5	27.3	13.5	0.41 ± 0.23
6	$1.7^{+0.4}_{-0.8}$	4.5	28.1	15.2	0.23 ± 0.08
7	$6.5^{+1.1}_{-1.4}$	3.2	28.4	13.5	0.19 ± 0.04
8	0	–	–	–	–
Weighted Avg.	–	–	–	–	0.158 ± 0.03

Table 4. Luminosity Results - Local Density

Field	Σ_{IPN} ($10^5 L_{\odot} \text{ kpc}^{-2}$)	Σ_{25} ($10^5 L_{\odot} \text{ kpc}^{-2}$)	Fraction ₂₅ ($\Sigma_{\text{IPN}} / \Sigma_{25} + \Sigma_{\text{IPN}}$)	Σ_{50} ($10^5 L_{\odot} \text{ kpc}^{-2}$)	Fraction ₅₀ ($\Sigma_{\text{IPN}} / \Sigma_{50} + \Sigma_{\text{IPN}}$)
2	8.4	4.2	0.67 ± 0.42	18.9	0.31 ± 0.20
3h	19.9	48.8	0.29 ± 0.04	23.4	0.46 ± 0.06
3l	4.5	48.8	0.08 ± 0.02	23.4	0.16 ± 0.05
4	8.3	7.7	0.52 ± 0.36	6.0	0.58 ± 0.41
5	9.5	11.1	0.46 ± 0.26	7.8	0.55 ± 0.31
6	4.5	41.4	0.10 ± 0.04	13.9	0.24 ± 0.08
7	3.2	15.9	0.17 ± 0.03	11.3	0.22 ± 0.04
8	0	–	–	–	–
Weighted Avg.	–	–	0.133 ± 0.02	–	0.218 ± 0.03

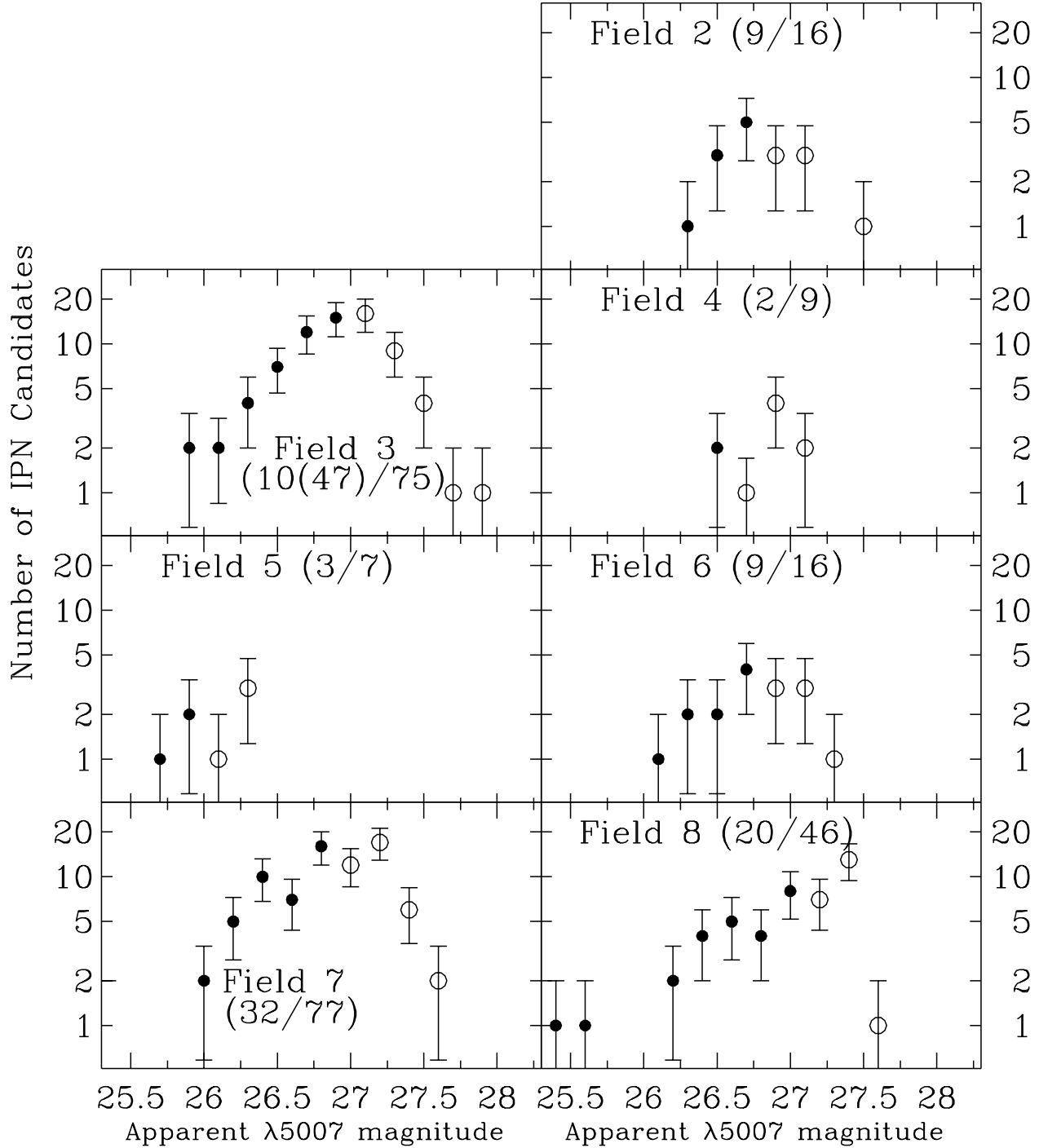


Fig. 1.— The luminosity functions of our IPN candidates, binned into 0.2 magnitude intervals. Filled points indicate objects brighter than our derived completeness limits from artificial star experiments, and open circles indicate objects fainter than the completeness limits. The numbers adjacent to each field show the number of IPN candidates above the completeness limits, and the total number of candidates.

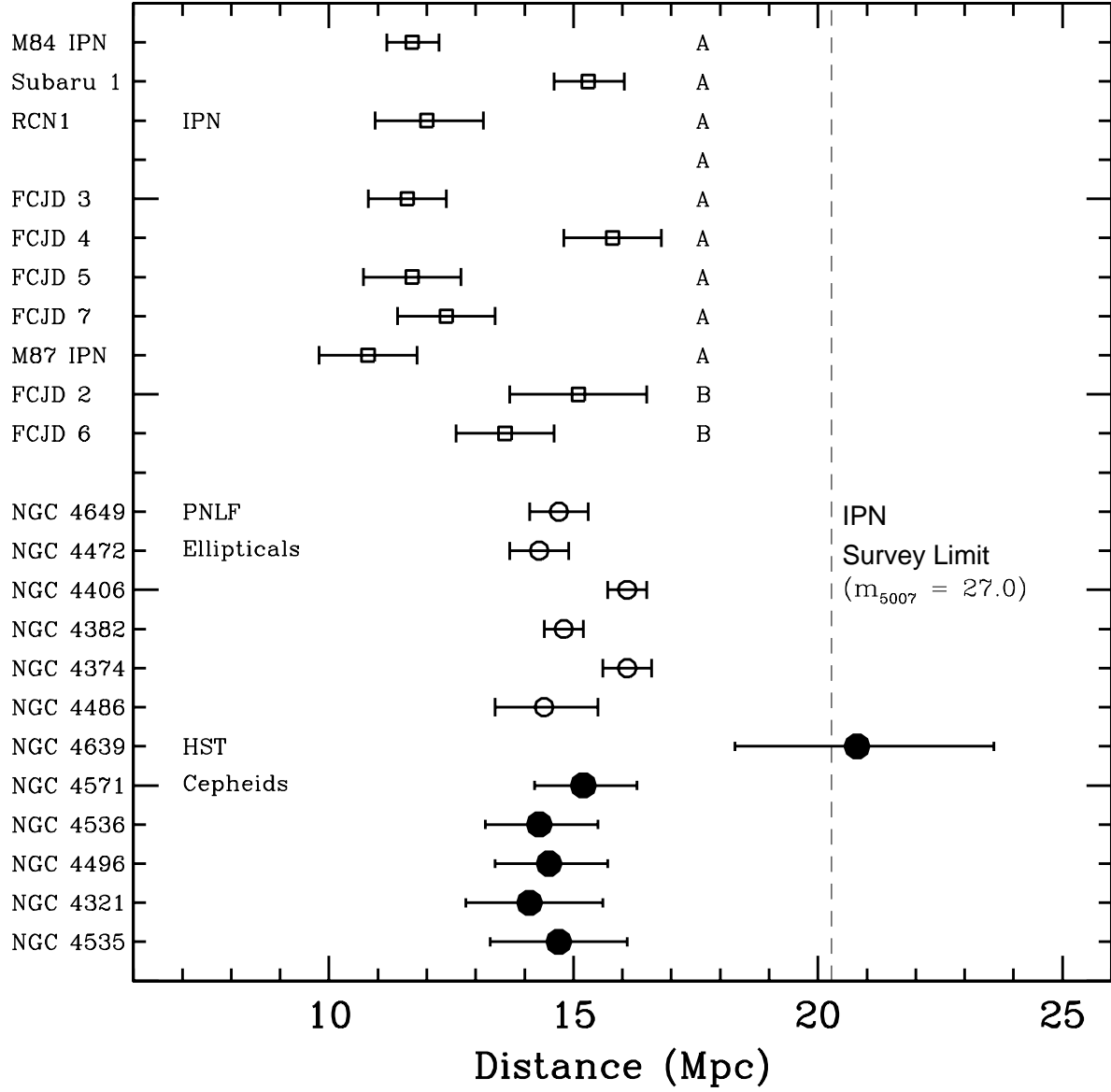


Fig. 2.— A comparison of the upper limit distances obtained from the intracluster planetary nebulae to direct distances to Virgo Cluster galaxies. At the top are the upper limit distances (denoted by the open squares) from IPN observations by Okamura et al. (2002) and Arnaboldi et al. (2002). Below that are the distances derived from the fields in Paper II, as well as the overluminous IPNe found in front of M87 (Ciardullo et al. 1998). These upper limit distances are compared to the PNLF distances of Virgo ellipticals (denoted by the open circles; Jacoby, Ciardullo, & Ford 1990; Ciardullo et al. 1998), and Cepheid distances to spiral galaxies (denoted by the filled circles; Pierce et al. 1994; Saha et al. 1997; Freedman et al. 2001). The subcluster of Virgo that each intracluster field resides in is noted. See the text for further discussion.

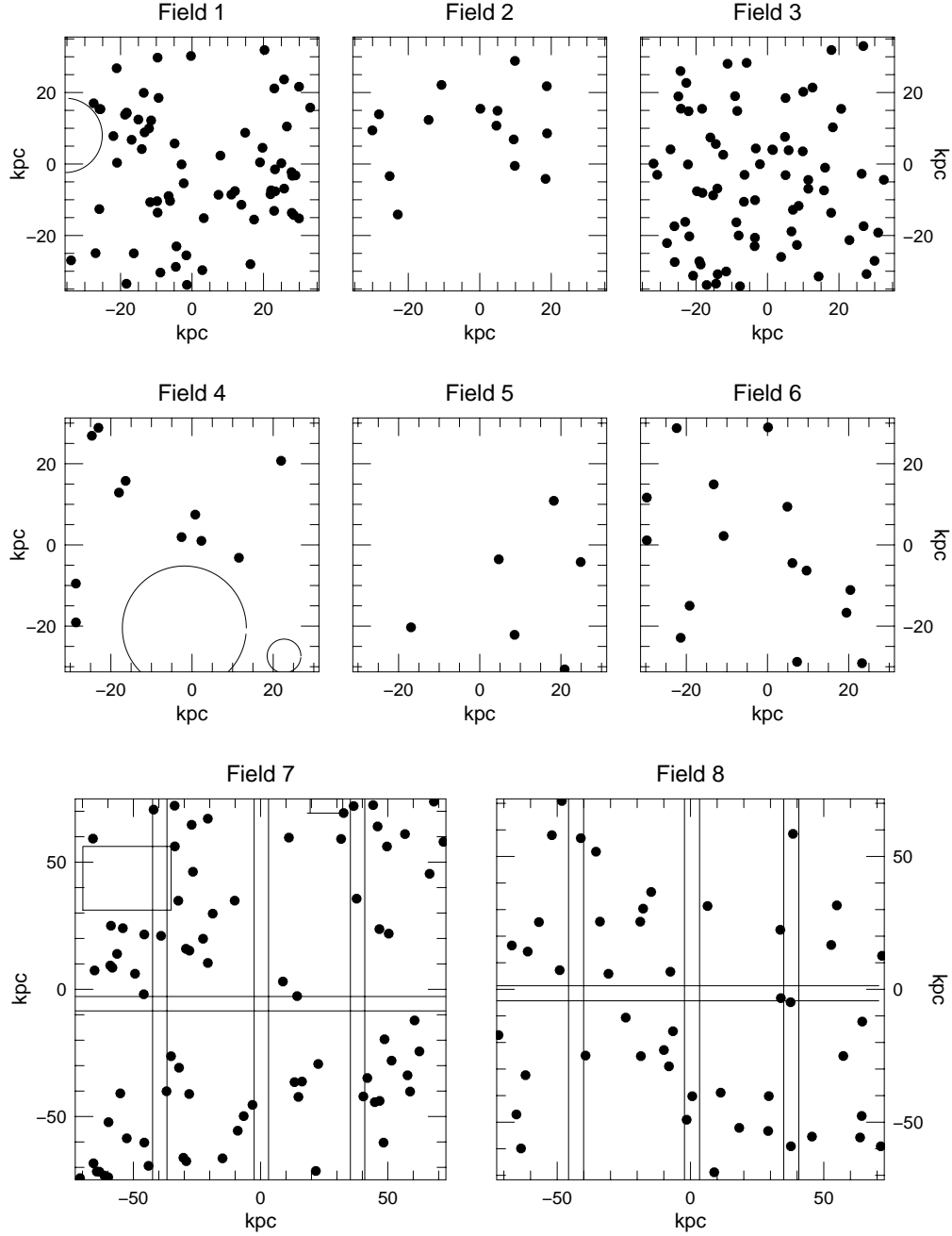


Fig. 3.— The distribution of IPN candidates on the sky, denoted as the filled circles. Fields 1–6 are the PFCCD fields, and Fields 7–8 are the MOSAIC fields. Field 1 is included for completeness. Large regions that were excluded from each field are noted by circles and rectangles. These include the regions between the MOSAIC CCD chips that are poorly surveyed and the areas around bright stars and galaxies. Note that there are no candidates in the bottom third of Field 2, a feature not seen in other fields, and the general clumpiness of the IPN distribution.

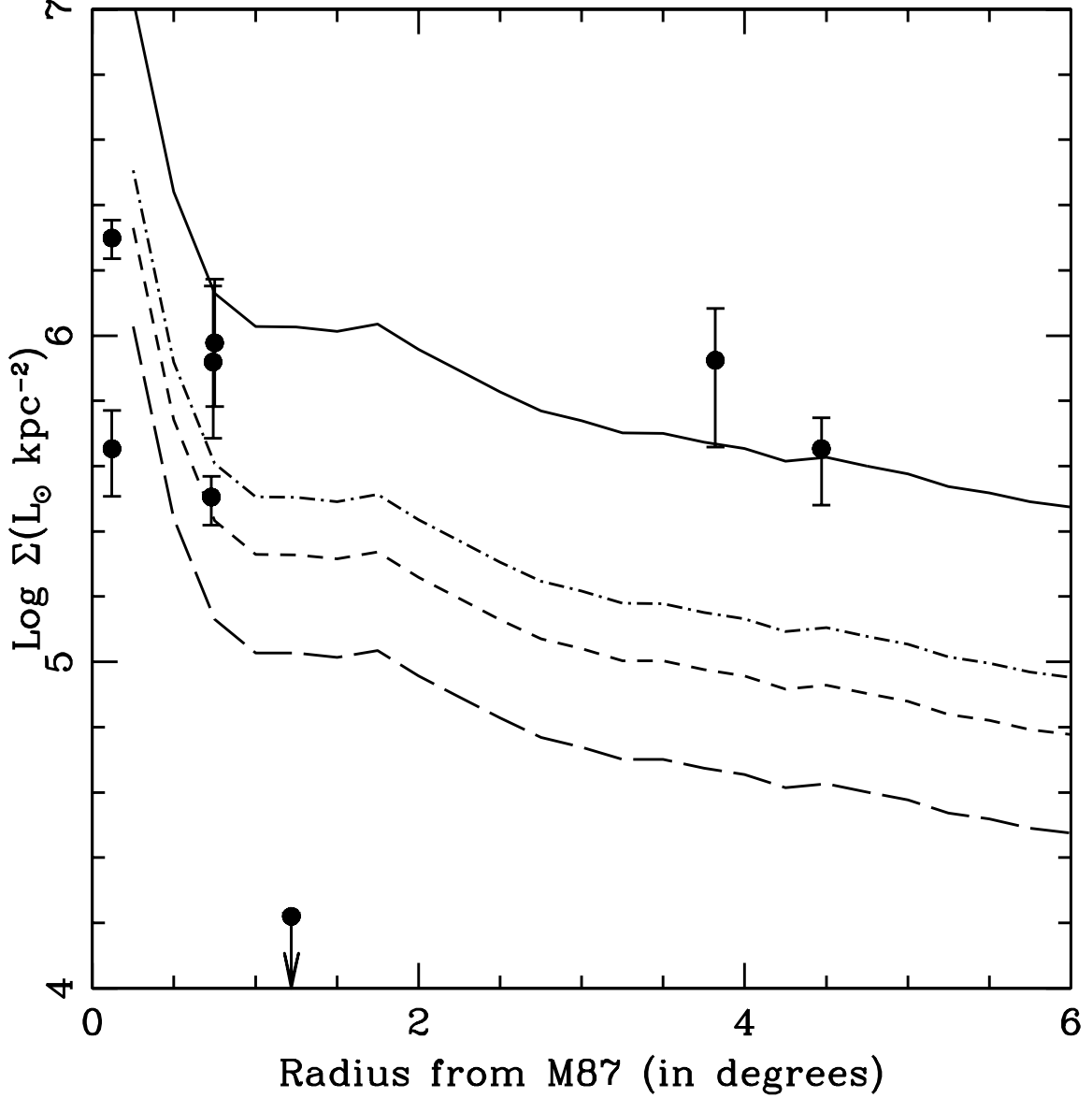


Fig. 4.— The radial distribution of Virgo’s intracluster light, derived from the IPN observations, compared to galaxy luminosity density. The solid line denotes the cluster’s cumulative luminosity density (see the text for how this quantity was calculated). The three dashed lines from bottom to top show the 10%, 20% and 30% fractions, respectively. Note that the decline of the IPN density is quite small compared to that of the galaxy light. Field 8, which has a density consistent with that of the background is denoted by the upper limit at $R \approx 1^\circ$

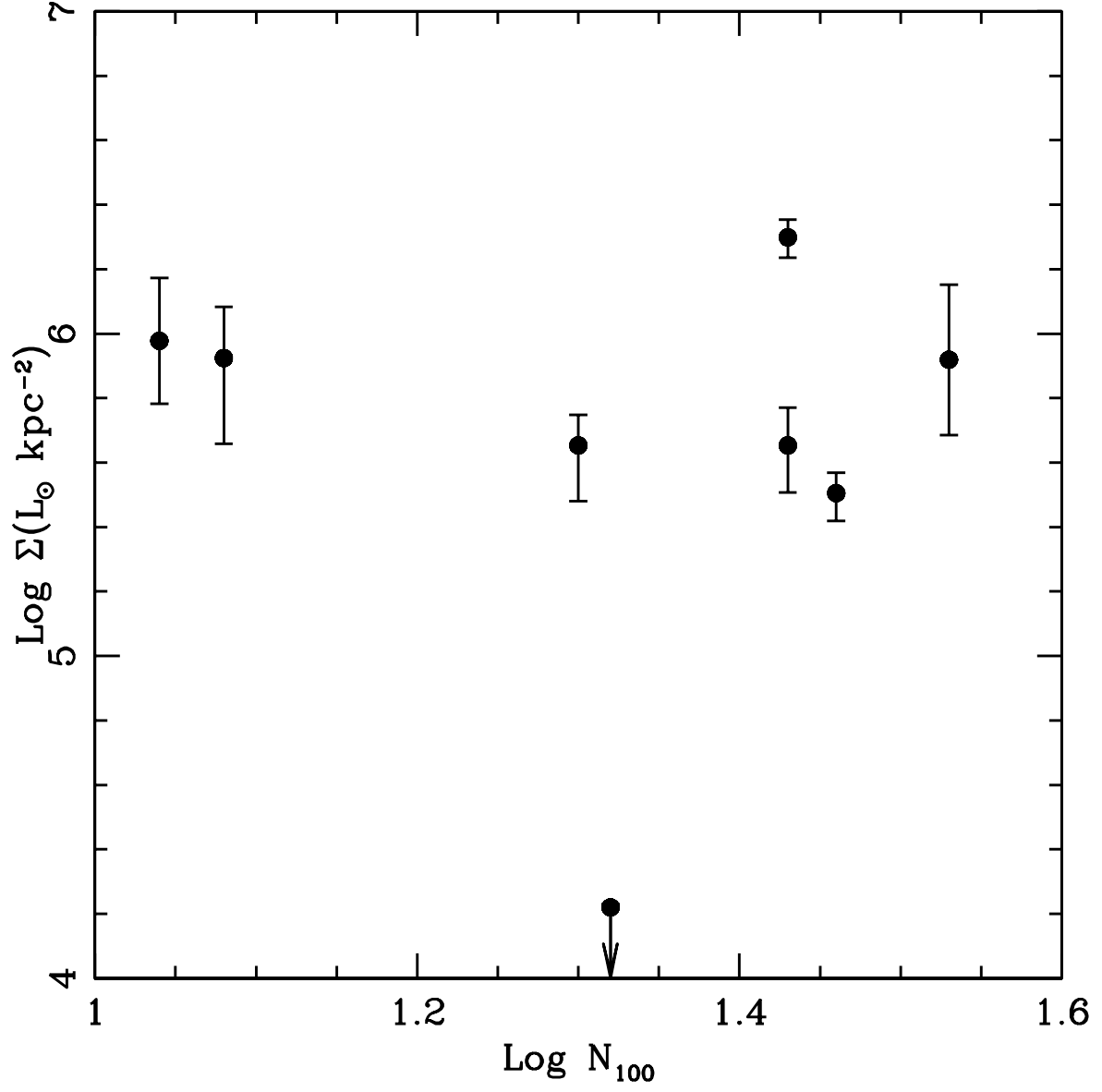


Fig. 5.— The density of intracluster light in Virgo, compared to local projected galaxy density within $100D_{15}$ kpc of each field. There appears to be little or no correlation with galaxy projected density. Field 8 has been given an upper limit, similar to Figure 4.